

Thermoelectric effects in a double quantum dot system weakly coupled to ferromagnetic leads

M. Bagheri Tagani, H. Rahimpour Soleimani,

Department of physics, University of Guilan, P.O.Box 41335-1914, Rasht, Iran

November 28, 2018

Abstract

Thermoelectric effects through a serial double quantum dot system weakly coupled to ferromagnetic leads are analyzed. Formal expressions of electrical conductance, thermal conductance, and thermal coefficient are obtained by means of Hubbard operators. Results show that although thermopower is independent of polarization of leads, figure of merit is reduced by increase of polarization. Influences of temperature and interdot tunneling on the figure of merit are also investigated, and observed that increase of the interdot tunneling strength results in reduction of the figure of merit. Effect of temperature on the thermal conductance is also analyzed.

1 Introduction

Thermopower through devices fabricated using nanotechnology has been increasingly studied in recent years [1, 2, 3, 4, 5, 6, 7, 8, 9, 10, 11]. Recent advances in the fabrication of nanodevices and the information showing nanodevices can work as thermal generators with high efficiency [12, 13, 14], have increased the importance of such studies. Indeed, violation of the Wiedemann-Franz law [15, 16], ratio of the electrical conductance to the thermal conductance is proportional to the operating temperature, in nanodevices results in increase of the thermal efficiency and the figure of merit, $ZT = \frac{S^2 G_V T}{\kappa}$, where S is the thermopower, G_V and T denote the electrical conductance and the temperature, respectively. $\kappa = \kappa_c + \kappa_{ph}$ is composed of the electrical and phonon thermal conductance, respectively. Discreteness of energy levels [17], Coulomb interactions [15, 18], interference effects [19], and so on lead to the fact that nanodevices have more thermal efficiency than bulky samples.

In recent years, investigation of the thermoelectrical devices fabricated from quantum dots (QDs) has attracted a lot of attention theoretically and experimentally [1, 2, 19, 20, 21, 22, 23, 24, 18, 25, 26]. However, thermoelectric effects through double quantum dots (DQDs) results in novel phenomena needing more studies. Few articles have analyzed thermopower through a DQD in just recent

years [27, 28, 29]. F. Chi and co-workers [28] showed ZT has two huge peaks in the vicinity of the electron-hole symmetry points. Trocha and J. Barnaś [29] reported ZT in DQD systems is enhanced due to Coulomb interactions and interference effects. We have recently studied [30] the effects of Coulomb interactions and interdot tunneling on the thermopower of a DQD system weakly coupled to metallic electrodes.

In this article, the influences of polarization of the leads, temperature, and interdot tunneling on the figure of merit and the thermoelectric conductances of a serial DQD weakly coupled to ferromagnetic leads are analyzed. Many-body representation introduced in Ref. [31] is used to obtain formal expressions for electrical and thermal conductances, thermopower, and figure of merit. Hamiltonian and model used for calculations are described in next section. Section 3 is devoted to numerical results and in the end, some sentences are given as conclusion.

2 Model and Method

We consider two single-level quantum dots coupled to ferromagnetic leads. Hamiltonian describing the system is given as

$$H = \sum_{\alpha k \sigma} \varepsilon_{\alpha k \sigma} c_{\alpha k \sigma}^\dagger c_{\alpha k \sigma} + \sum_{i \sigma} \varepsilon_i n_{i \sigma} + \sum_i U_i n_{i \uparrow} n_{i \downarrow} + U_{12} \sum_{\sigma \sigma'} n_{L \sigma} n_{R \sigma'} \quad (1)$$

$$+ t \sum_{\sigma} [d_{L \sigma}^\dagger d_{R \sigma} + H.C.] + \sum_{\alpha k \sigma} [V_{\alpha k \sigma} c_{\alpha k \sigma}^\dagger d_{\alpha \sigma} + H.C.]$$

where $c_{\alpha k \sigma}$ ($c_{\alpha k \sigma}^\dagger$) destroys (creates) an electron with spin σ , wave vector k , in lead $\alpha = L, R$. Energy levels of the leads are spin-dependent because the leads are ferromagnetic. The second and third terms in the above equation describe each dot. $d_{i \sigma}$ ($d_{i \sigma}^\dagger$) is annihilation (creation) operator of the i 'th ($i = L, R$) dot and $n_{i \sigma} = d_{i \sigma}^\dagger d_{i \sigma}$. Energy levels of each dot are assumed to be degenerate. U_i and U_{12} denote, respectively, on-site and interdot Coulomb repulsions. t is the interdot tunneling strength, whereas $V_{\alpha k \sigma}$ denotes the dot-lead coupling strength. In order to study the system, the Hubbard operators have been used. In this model, the Hamiltonian of the isolated DQD system is diagonalized and the creation and annihilation operators are expanded in terms of obtained eigenstates. It is obvious that the system has 16 different states shown as $|N, n \rangle$ where $N = 0 \dots 4$ is the number of electrons, whereas n denotes n 'th state of N -electron configuration. By expanding annihilation operator as

$$d_{\alpha \sigma} = \sum_{N n n'} (d_{\alpha \sigma})_{N N+1}^{n n'} X_{N N+1}^{n n'} \quad (2)$$

where the Hubbard operator, $X_{N N+1}^{n n'} = |N n \rangle \langle N + 1 n'|$, describes a transition in which an electron inside the DQD system is annihilated, the whole

Hamiltonian is given as

$$H = \sum_{\alpha k \sigma} \varepsilon_{\alpha k \sigma} c_{\alpha k \sigma}^\dagger c_{\alpha k \sigma} + \sum_{Nn} E_{Nn} h_N^n + \sum_{\alpha k \sigma N n n'} [V_{\alpha k \sigma} (d_{\alpha \sigma})_{NN+1}^{nn'} c_{\alpha k \sigma}^\dagger X_{NN+1}^{nn'} + H.C] \quad (3)$$

where $h_N^n = |Nn \rangle \langle Nn|$.

Now, population number P_{Nn} , the probability of being in the state $|Nn \rangle$, is computed by means of density matrix approach. Coupling to the leads is considered so weak that non-diagonal elements of the density matrix are ignored because they are proportional to $V_{\alpha k \sigma}^4$. Using Markov approximation and wide band limit, the time evaluation of the population numbers is given as [31]

$$\frac{dP_{01}}{dt} = \sum_{\alpha n} [-\Gamma_{|01\rangle \rightarrow |1n\rangle}^\alpha P_{01} + \Gamma_{|1n\rangle \rightarrow |01\rangle}^\alpha P_{1n}] \quad (4a)$$

$$\begin{aligned} \frac{dP_{Nn}}{dt} = \sum_{\alpha n'} & -[\Gamma_{|Nn\rangle \rightarrow |N-1n'\rangle}^\alpha + \Gamma_{|Nn\rangle \rightarrow |N+1n'\rangle}^\alpha] P_{Nn} + \\ & \Gamma_{|N-1n'\rangle \rightarrow |Nn\rangle}^\alpha P_{N-1n'} + \Gamma_{|N+1n'\rangle \rightarrow |Nn\rangle}^\alpha P_{N+1n'} \end{aligned} \quad (4b)$$

$$\frac{dP_{41}}{dt} = \sum_{\alpha n} [-\Gamma_{|41\rangle \rightarrow |3n\rangle}^\alpha P_{41} + \Gamma_{|3n\rangle \rightarrow |41\rangle}^\alpha P_{3n}] \quad (4c)$$

It is obvious that there is one configuration for zero- and four-electron state. The transition rates are

$$\Gamma_{|Nn\rangle \rightarrow |N+1n'\rangle}^\alpha = \frac{1}{\hbar} \sum_{\sigma} \Gamma_{\sigma}^\alpha |(d_{\alpha \sigma})_{NN+1}^{nn'}|^2 f_{\alpha}(E_{N+1n'} - E_{Nn}) \quad (5a)$$

$$\Gamma_{|N+1n'\rangle \rightarrow |Nn\rangle}^\alpha = \frac{1}{\hbar} \sum_{\sigma} \Gamma_{\sigma}^\alpha |(d_{\alpha \sigma})_{NN+1}^{nn'}|^2 f_{\alpha}^{-}(E_{N+1n'} - E_{Nn}) \quad (5b)$$

where $\Gamma_{\sigma}^\alpha = 2\pi \sum_{k \in \alpha} |V_{\alpha k \sigma}|^2$ is the spin-dependent tunneling rate, $f_{\alpha}(x) = (1 + \exp((x - \mu_{\alpha})/kT_{\alpha}))^{-1}$ is the Fermi-Dirac distribution function in which μ_{α} and T_{α} stand for the chemical potential and the operating temperature of the lead α , respectively, and $f_{\alpha}^{-} = 1 - f_{\alpha}$. The charge and energy currents are computed by solving the Eqs. (4) in the steady state situation ($\frac{dP_{Nn}}{dt} = 0$)

$$I^{\alpha} = -e \sum_{N, N', n, n'} \Gamma_{|Nn\rangle \rightarrow |N'n'\rangle}^{\alpha} P_{|Nn\rangle} \text{sgn}(N' - N) \quad (6a)$$

$$Q^{\alpha} = \sum_{N, N', n, n'} \Gamma_{|Nn\rangle \rightarrow |N'n'\rangle}^{\alpha} (E_{|N'n'\rangle} - E_{|Nn\rangle}) P_{|Nn\rangle} \text{sgn}(N' - N) \quad (6b)$$

where $\text{sgn}(x)$ is a signum function.

To compute the thermoelectrical characteristics of the system, the linear response regime is used. We assume that the left lead is slightly hotter than the right one ($T_L = T_R + \Delta T$), and $\mu_L = \mu_R - e\Delta V$, so that the charge and energy currents are given as follows

$$I^{\alpha} = G_V \Delta V + G_T \Delta T \quad (7a)$$

$$Q^{\alpha} = M \Delta V + K \Delta T \quad (7b)$$

where G_V is the electrical conductance and G_T is the thermal coefficient. Thermopower is defined as minus ratio of induced voltage to applied temperature gradient under condition that the charge current is zero, so we have $S = \frac{G_T}{G_V}$. Putting $I^L = 1/2(I^L - I^R)$ and expanding the fermi-Dirac distribution function as $f_L(x) = f_R(x) - x/T f'(x)\Delta T + e\Delta V f'(x)$ where $f'(x) = \partial f(x)/\partial x$, one can easily obtain:

$$G_V = -\frac{e^2}{2\hbar} \sum_{Nnn'} \sum_{\sigma} P_{Nn} \Gamma_{\sigma}^L [|(d_{L\sigma})_{NN+1}^{nn'}|^2 f'(E_{N+1n'} - E_{Nn}) + |(d_{L\sigma})_{N-1N}^{n'n}|^2 f'(E_{Nn} - E_{N-1n'})] \quad (8a)$$

$$G_T = \frac{e}{2\hbar} \sum_{Nnn'} \sum_{\sigma} P_{Nn} \Gamma_{\sigma}^L [|(d_{L\sigma})_{NN+1}^{nn'}|^2 \frac{(E_{N+1n'} - E_{Nn})}{T} f'(E_{N+1n'} - E_{Nn}) + |(d_{L\sigma})_{N-1N}^{n'n}|^2 \frac{(E_{Nn} - E_{N-1n'})}{T} f'(E_{Nn} - E_{N-1n'})] \quad (8b)$$

Using above equations and Onsager relation, the thermal conductance is computed as [17]

$$\kappa_c = [K - S^2 G_V T] \quad (9)$$

where

$$K = -\frac{1}{2\hbar} \sum_{Nnn'} \sum_{\sigma} P_{Nn} \Gamma_{\sigma}^L [|(d_{L\sigma})_{NN+1}^{nn'}|^2 \frac{(E_{N+1n'} - E_{Nn})^2}{T} f'(E_{N+1n'} - E_{Nn}) + |(d_{L\sigma})_{N-1N}^{n'n}|^2 \frac{(E_{Nn} - E_{N-1n'})^2}{T} f'(E_{Nn} - E_{N-1n'})] \quad (10)$$

For simulation purpose, we assume that $\Gamma_{\uparrow}^L = \Gamma_{\uparrow}^R = \Gamma_0$ and spin-down tunneling rate is equal to $\Gamma_{\downarrow}^L = \Gamma_{\downarrow}^R = \alpha\Gamma_0$ where $0 \leq \alpha \leq 1$. It is obvious that $\alpha = 1$ denotes normal metallic electrodes whereas $\alpha = 0$ stands for half-metal leads. we also set $\kappa_{ph} = 3\kappa_0$ where $\kappa_0 = \frac{\pi^2 k_B^2}{3\hbar} T$ is the quantum of thermal conductance [32] and, assume that the single electron levels in the QDs are degenerate. In recent years, the phonon contribution in the transport through QDs has been extensively studied experimentally and theoretically [33, 34, 35].

3 Results and discussions

Figure of merit (ZT) as a function of the QDs' energy level and the temperature is plotted in fig. 1 for different α s. Similar plot was previously presented in Ref. [18] about a QD coupled to Ferromagnetic electrodes or in Ref.[29] about a DQD coupled to external electrodes. One can observe that increasing α results in the reduction of ZT . On the other hand, ZT has some peaks whose intensities decrease with increase of temperature, but become wider. The results also show

that ZT approaches zero in $-3 < \varepsilon_i < 0$ and high temperature ($T > 4k$). With respect to the fact that ZT is a function of the Seebeck coefficient, the electrical conductance, and the thermal conductance, the evaluation of them will help us realize the behavior of ZT .

Figure. 2a describes the electrical conductance as a function of the energy level in different situations. From eq. (8a) it is obvious that G_V has a peak whenever the necessary energy for transition from N -electron state to $N \pm 1$ -electron state equals to the Fermi energy of the leads ($\mu_\alpha = 0$). In low temperature ($T = 2k$), $f'(x)$ is a Lorentzian function with narrow width, thus the peaks and the Coulomb valleys are clearly observed. There are four peaks because four electron can exist in the system. With increase of the temperature, the intensity of the peaks reduces whereas they become wider. Furthermore, the Coulomb valleys are vanished because increase of the temperature weakens the Coulomb blockade effect. It is straightforward to show that $G_V = \frac{1+\alpha}{2}G_0$ where G_0 is the electrical conductance of a double quantum dot coupled to normal metal electrodes. Therefore, the polarized electrodes decrease the electrical conductance of the system. The thermal coefficient as a function of energy is shown in fig. 2b. One can easily observe from eq.(8b), for energies in which G_V has a maximum G_T and as result, S become zero because of $E_{Nn} \approx E_{N\pm 1n'}$. In these energy points, although the transition from N -electron state to $N \pm 1$ -electron state results in the electrical current, no net energy transports in the process. Indeed, the temperature gradient does not have any significant role in producing the charge current in resonance energies. In addition, the thermal coefficient becomes zero in some other energies. From eq.(8b), it is obvious when the system is in a certain state ($P_{Nn} \simeq 1$) and $E_{N+1n'} - E_{Nn} = -(E_{Nn} - E_{N-1n'})$, then $G_T = 0$. These energy points are so-called electron-hole symmetry points and the effect has been recently studied in a multilevel QD [36]. In symmetry points, the current transported from the lead to the QD is equal to the current transported in opposite direction, so that the thermopower becomes zero. Indeed, both electrons and holes participate in producing the current with different signs. It is worth noting that G_T goes from positive to negative values in resonance points whereas it behaves reversely in symmetry points. This effect, bipolar effect, has been recently reported in a multilevel quantum dot [36]. It comes from the fact that in each side of it, a kind of charge carrier (electron or hole) participates in transport. This leads to the oscillation of the thermopower. Increasing temperature gives rise to widening G_T but its intensity will be reduced. The influence of the polarization of the leads on the thermal coefficient is the same as G_V and as a result, the thermopower is independent of the α . This result was previously reported about a single level QD coupled to ferromagnetic leads [20]. However, results presented in Ref. [18] show that the thermopower weakly depends on the polarization of the leads. This difference comes from the different models used for studying the system. Indeed, in nonequilibrium Green's function formalism used in Ref. [18], the broadening of the QD level due to coupling between the QD and the leads is taken into account. That leads to the dependence of the thermopower on the magnetic polarization. In rate equations approach, the broadening of the

QD level due to coupling is disregarded. Figure of merit is zero in resonance and symmetry points as one can see in fig. 1 due to $ZT \propto S$. Furthermore, ZT decreases with increase of temperature because increasing temperature results in reducing S and G_V . On the other hand, although the thermopower is spin-independent, the figure of merit is reduced by increase of polarization because of $ZT \propto G_V$.

The thermal conductance as a function of temperature and energy level is shown in fig. 3. Results show that the thermal conductance takes the highest values in electron-hole symmetry points when the temperature is sufficiently high. In these points, electrons and holes participate in the transfer of charge and heat with the same weight. Because the current carried by holes is in the opposite direction with one carried by electrons, the charge current becomes zero in these energies so that one can observe as valleys of G_V in fig. 2a. In contrast with the charge current, electrons and holes carry the energy in the same direction resulting in the appearance of the peaks in κ_c . As expected, increasing temperature gives rise to the increase of κ_c . In low temperature, the peaks of G_V and κ_c are happened in nearly same energies. Indeed, the significant difference between G_V and κ_c is observed in high temperature. In low temperature, when the transition energy is equal to resonant energy, one peak develops in both G_V and κ_c , resulting due to the transfer of current and heat through the system by electrons [18, 29].

Figure. 4 describes figure of merit as a function of the polarization of the leads and the interdot tunneling strength. It is observed that increase of the polarization of the leads results in the reduction of ZT . Results also show that the interdot tunneling leads to decrease of ZT . Indeed, From fig. 4 one can approximately consider $ZT \propto \alpha t$ so that ZT obtained from strong α (weak polarization) and weak t is equal to result obtained from weak α (strong polarization) and strong t . It is important to note that the eigenvalues of the DQD are a function of the interdot tunneling, so the position of symmetry and resonance points depends on the interdot tunneling strength. It is worth noting that increase of interdot tunneling results in reduction of G_V [30]. Furthermore, although the thermopower is spin-independent, the electrical conductance is reduced by increasing polarization, and as a result the figure of merit reduces when the polarization of leads increases. In addition, intra- and interdot Coulomb repulsions affect the figure of merit significantly. Recently, we have shown that the increase of Coulomb repulsion results in the increase of figure of merit [30]. Indeed, the level spacing is increased by increase of Coulomb repulsion and as a result, the bipolar effect will be reduced. The same effect was previously reported about a multilevel QD [36].

4 Conclusion

In this paper, the thermopower in a serial double quantum dot system weakly coupled to ferromagnetic leads is studied using Hubbard operators. Formal expressions for thermal conductance, electrical conductance, and thermal coef-

ficient are obtained using density matrix approach. The effect of temperature, interdot tunneling, and polarization of leads on the thermoelectrical characteristics of the system is examined. Results show that increase of temperature results in decrease of electrical conductance intensity whereas it becomes wider. It is found that although the thermopower is independent of polarization, the figure of merit is reduced by increase of polarization. Influence of the interdot tunneling on the figure of merit is also analyzed.

References

- [1] Y. Dubi and M. Di Ventra, *Rev. Mod. Phys* 83 (2011) 131.
- [2] A.V. Andreev, K. A. Matveev, *Phys. Rev. Lett.* 86 (2001) 280.
- [3] D. Vashaee and A. Shakouri, *Phys. Rev. Lett.*, 92 (2004) 106103.
- [4] C. M. Finch, V. M. García-Suárez, C. J. Lambert, *Phys. Rev. B* 79 (2009) 033405.
- [5] Y. Dubi and M. Di Ventra, *Phys. Rev. B* 79 (2009) 115415.
- [6] C. Bera, M. Soulier, C. Navone, G. Roux, J. Simon, S. Volz, N. Mingo, *J. Appl. Phys.* 108 (2010) 124306.
- [7] D. Nozaki, H. Sevinli, W. Li, R. Gutierrez, G. Cuniberti, *Phys. Rev. B* 81 (2010) 235406.
- [8] D. M.-T. Kuo, and Y-C. Chang, *Phys. Rev. B* 81 (2010) 205321.
- [9] C. P. Moca, A. Roman, D. C. Marinescu, *Phys. Rev. B* 83 (2011) 245308.
- [10] D. Singh, J. Y. Murthy, T. S. Fisher, *J. Appl. Phys* 110 (2011) 044317.
- [11] A. I. Hochbaum, R. Chen, R. D. Delgado, W. Liang, E. C. Garnett, M. Najarian, A. Majumdar, P. Yang, *Nature*, 451 (2008) 163.
- [12] A. A. Balandin, O. L. Lazarenkova, *Appl. Phys. Lett.* 82 (2003) 415.
- [13] A. Khitun, A. Balandin, K.L. Wang, G. Chen, *Physica E*, 8 (2000) 13.
- [14] F. Mazzamuto, V. Hung Nguyen, Y. Apertet, C. Caër, C. Chassat, J. Saint-Martin, P. Dollfus, *Phys. Rev. B* 83 (2011) 235426.
- [15] B. Kubala, J. König, J. Pekola, *Phys. Rev. Lett.* 100 (2008) 066801.
- [16] A. Garg, D. Rasch, E. Shimshoni, A. Rosch, *Phys. Rev. Lett.* 103 (2009) 096402.
- [17] X. Zianni, *Phys. Rev. B* 78 (2008) 165327.
- [18] R. Świrkowicz, M. Wierzbicki, J. Barnaś, *Phys. Rev. B* 80 (2009) 195409.

- [19] Y. S. Liu, D. B. Zhang, X. F. Yang, J. F. Feng, *Nanotechnology* 22 (2011) 225201.
- [20] Y Dubi, M. Di Ventra, *Phys. Rev. B* 79 (2009) 081302R.
- [21] Y. Xu, X. Chen, J-S. Wang, B-L. Gu, W. Duan, *Phys. Rev. B* 81 (2010) 195425.
- [22] Y, Ying, G. Jin, *Appl. Phys. Lett.* 96 (2010) 093104.
- [23] Y. Ahmadian, G. Catelani, I. L. Aleiner, *Phys. Rev. B* 72 (2005) 245315.
- [24] T. A. Costi, V. Zlatić, *Phys. Rev. B* 81 (2010) 235127.
- [25] M. Galperin, A. Nitzan, M. A. Ratner, *Phys. Rev. B* 75 (2007) 155312.
- [26] A. Tan, S. Sadat, P. Reddy, *Appl. Phys. Lett.* 96 (2010) 013110.
- [27] Z-Y. Zhang, *J. Phys: Condensed matter*, 19 (2007) 086214.
- [28] F. Chi, J. Zheng, X. D. Lu, K. C. Zhang, *Phys. Lett. A*, 375 (2011) 1352.
- [29] P. Trocha, J. Barnaś, arXiv:1108.2422v1, (2011).
- [30] M. B. Tagani, H. R. Soleimani, *Physica B* 407 (2012) 765.
- [31] J. Fransson, M.R'asander, *Phys. Rev. B*, 73 (2006) 205333.
- [32] L. G. C. Rego, G. Kirczenow, *Phys. Rev. Lett.* 81 (1998) 232.
- [33] B.J. LeRoy, S.G. Lemay, J. Kong, and C. Dekker, *Nature*, 432 (2004) 371.
- [34] A. K. Hüttel, B. Witkamp, M. Leijnse, M. R. Wegewijs, H. S. J. van der Zant, *Phys. Rev. Lett.* 102 (2009) 225501.
- [35] M, Galperin, M. A. Ratner, A. Nitzan, *J. Phys.: Condens. Matter* 19 (2007) 103201.
- [36] J. Liu, Q. F. Sun, X. C. Xie, *Phys. Rev. B*, 81 (2010) 245323.

Figure captions

Figure. 1: Color map of figure of merit. Parameters are: $t = 0.2meV$, $U_i = 2meV$, $U_{12} = 1meV$ and $\Gamma_0 = 10\mu eV$.

Figure. 2: G_V and G_T as a function of energy. Solid ($T = 2K, \alpha = 1$), dashed ($T = 5K, \alpha = 1$), dash-dotted ($T = 2K, \alpha = 0.5$), and dotted ($T = 5K, \alpha = 0.5$). Other parameters are the same as fig. 1 .

Figure. 3: Color map of thermal conductance. Parameters are the same as fig. 1.

Figure. 4: Figure of merit as a function of polarization and interdot tunneling. Parameters are the same as fig. 1 except $T = 2K$ and $\varepsilon_i = -1.5meV$.

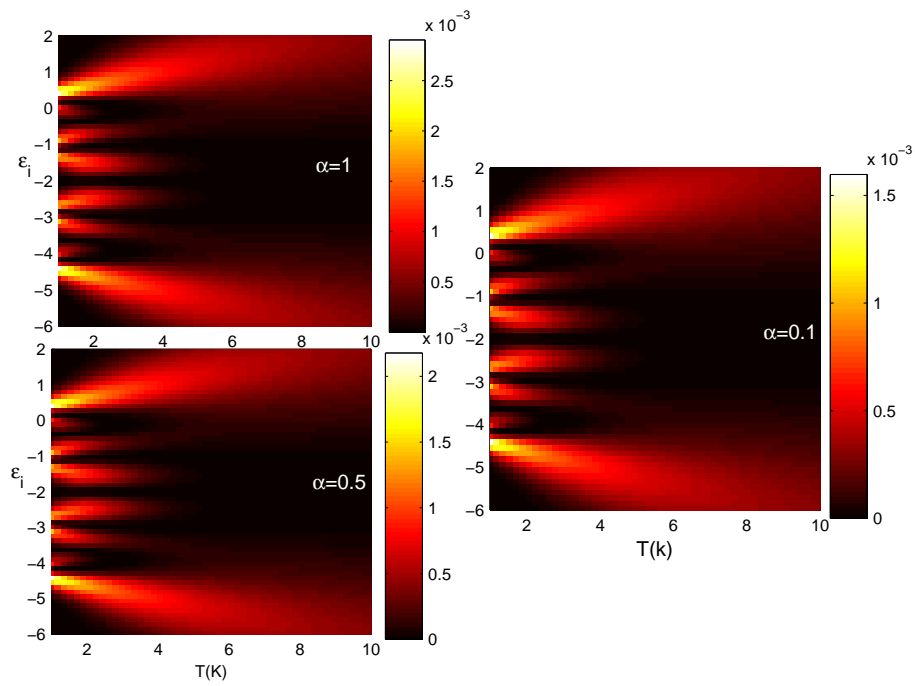


Figure.1

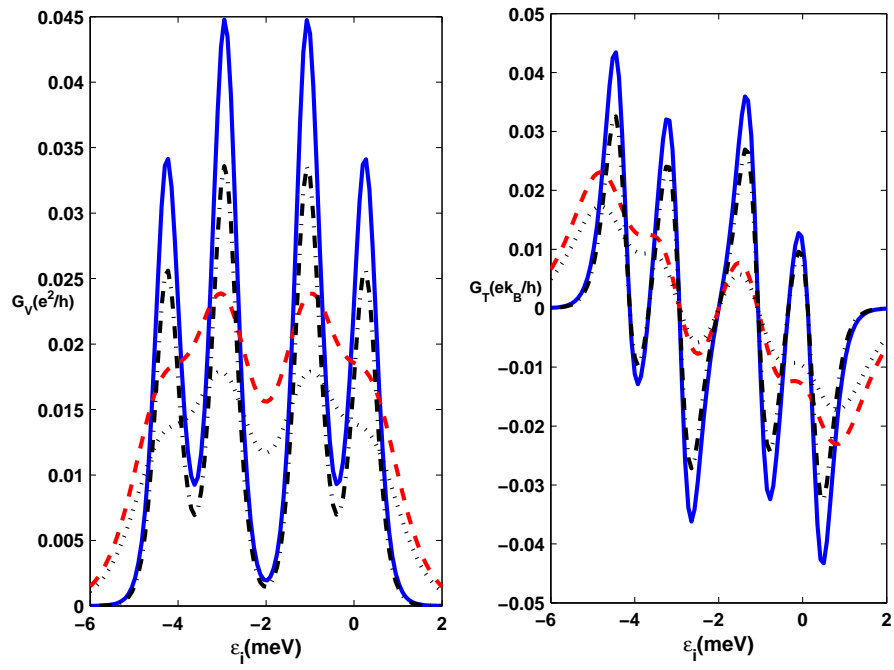


Figure.2

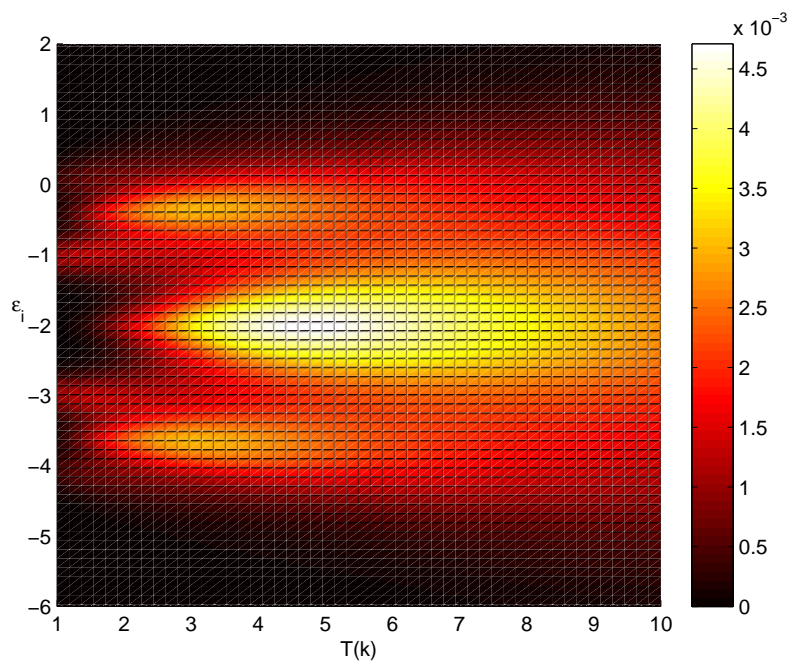


Figure.3

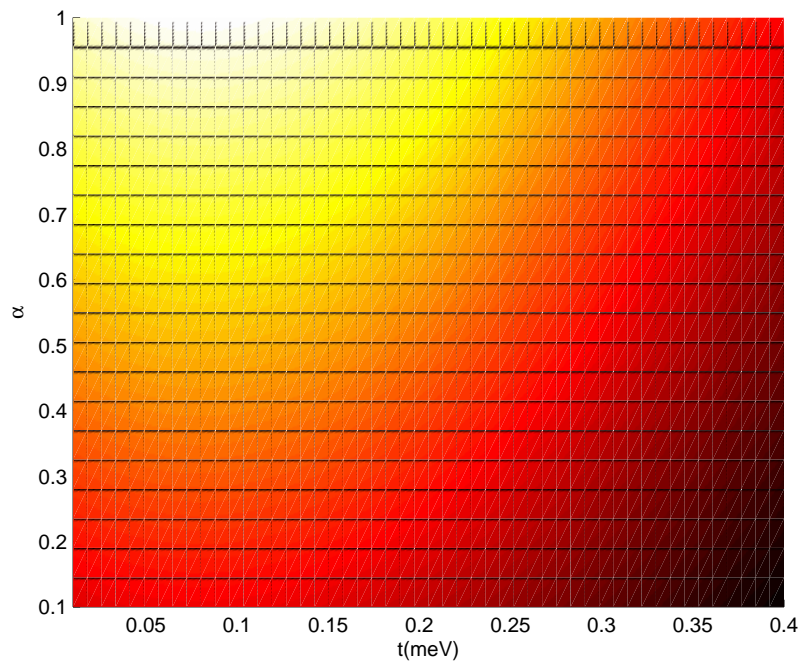


Figure.4